Volume 14, Number 4, 2021. pp. 359-378

Jordan Journal of Physics

ARTICLE

Retrieval of Optical Constants of Undoped Flash-Evaporated Lead Iodide Films from an Analysis of Their Normal Incidence Transmission Spectra Using Swanepoel's Transmission Envelope Theory of Non-Uniform Films

Mousa M. A-G. Jafar[a], **Nidal M. Ershaidat**[a], **Mais J. A. Ahmad**[b], **Mahmoud H. Saleh**[c] and **Basim N. Bulos**[a]

[a] *Department of Physics, School of Science, The University of Jordan, Amman 11942, Jordan.*

[b] *Leibniz Institute für Analytische Wissenschaften-ISAS e. V., Bunsen-Kirchhoff-Straße 11, D-44139 Dortmund, Germany.*

[c] *Department of Physics, Faculty of Science, Al-Balqa Applied University, Al-Salt 19117, Jordan.*

Doi: **https://doi.org/10.47011/14.4.10**

Received on: 17/09/2020; *Accepted on: 12/01/2021*

Abstract: Normal-incidence transmission-wavelength ($T_{\mathrm{exp}}(\lambda)-\lambda$) spectra of 1 and 1.2 μm thick flash-evaporated lead iodide (PbI_2) films on 1.1 mm thick glass slides held at 200 °C display well-spaced several interference-fringe maxima and minima in the λ-range 520-900 nm, without exhibiting a transparent region and with the maxima lying well below the substrate transmission. Below 520 nm, these $T_{\mathrm{exp}}(\lambda)-\lambda$ curves drop steeply to zero (at $\lambda \lesssim 505$ nm), signifying crystalline-like PbI_2 film absorption. As corrections of measured (PbI_2 film/substrate) transmittance data for substrate absorption and spectrometer slit-width effect were marginal over the studied λ-range, the observed low transmittance of (PbI_2 film/substrate) system was related to PbI_2 film thickness non-uniformity (Δd), which causes shrinkage of both maxima and minima and leads to significant film optical absorption that reduces both maxima and minima. The McClain ENVELOPE algorithm was utilized, with a minor modification, to construct maxima $T_{\mathrm{M}}(\lambda_{\max}/\lambda_{\min})$ and minima $T_{\mathrm{m}}(\lambda_{\min}/\lambda_{\max})$ envelope curves, which were analyzed by Swanepoel's envelope method of non-uniform films using an approach that takes account of dispersive substrate refractive index $n_{\mathrm{s}}(\lambda)$ and circumvents the non-availability of a high-λ transparency region. In such analytical approach, Δd was varied till a re-generated $T_{\mathrm{gen}}(\lambda)-\lambda$ curve matches the $T_{\mathrm{exp}}(\lambda)-\lambda$ curve. An average thickness $\bar{d}$ of the film, besides its refractive index $n(\lambda)$ and absorption coefficient $\alpha(\lambda)$ in the weak, medium and strong absorption regions, were then obtained. The energy-dependence of $\alpha(\lambda)$ is discussed in view of interband electronic transition models. The obtained results are consistent with other literature studies on similar flash-evaporated PbI_2 films.

Keywords: PbI_2, Optical constants and bandgap, Swanepoel's transmission envelope method, Non-uniform films.

Corresponding Author: Mousa M. Abdul-Gader Jafar **Email**: mousa_jafar_2030@yahoo.com

Introduction

Single crystals and films of lead iodide (PbI_2) have emerged to be prospective candidates for use in many electronic devices, including room-temperature radiation detectors and x-ray imaging systems [1-3] and in perovskite solar-cell photovoltaics and photodetectors [4-6]. This is because PbI_2 has useful structural, electrical and optical properties [7-18]. The quality and properties of a PbI_2 film depend on its purity, stoichiometry, crystallinity and homogeneity, which are governed by the used fabrication route. Crystals/films of lead iodide can be prepared from solution, vapor, gel and melt at different temperatures up to its melting point (~ 410 °C) [7-21].

An accurate and reliable determination of optical constants and thickness of semiconducting films is of importance for basic understanding of their optical and dielectric properties and for the design, fabrication and development of electronic devices integrating them. The refractive index and extinction coefficient of a material sample are common optical constants that are valuable for explicating its optical/dielectric behavior and dissipation under various experimental conditions. However, their measurement is not straightforward, but can be retrieved from a measurable macroscopic physical quantity of the specimen, such as its transmittance $T(\lambda)$ and/or reflectance $R(\lambda)$ that can be measured directly using spectrophotometers as a function of wavelength λ of quasi-monochromatic light incident upon it.

As the transmittance or reflectance of a material film is not an inherent material property, one has to analyze its $T_{\text{exp}}(\lambda)-\lambda$ and/or $R_{\text{exp}}(\lambda)-\lambda$ data to determine the real $n(\lambda)$ and imaginary $\kappa(\lambda)$ components of its complex refractive index $\hat{n}(\lambda)=n(\lambda)-i\,\kappa(\lambda)$ as a function of λ. The $\kappa(\lambda)$ data can be used to find its optical absorption coefficient $\alpha(\lambda)$ and *vice versa* using the relation $\alpha(\lambda)\equiv 4\pi\kappa(\lambda)/\lambda$. This requires mathematical formulae for $T(\lambda)$ or $R(\lambda)$ that incorporate $n(\lambda)$ and $\kappa(\lambda)$ and a method for analyzing $T_{\text{exp}}(\lambda)-\lambda$ and $R_{\text{exp}}(\lambda)-\lambda$ data using such formulae, which depend on the type of optical system. Here, we will be concerned with an optical system in the form of an absorbing film on a thicker slab (substrate), immersed in air ($n_a(\lambda)=1$ and $\kappa_a(\lambda)$=0).

Theoretical formulae that describe $T(\lambda)$ or $R(\lambda)$ of an absorbing slab of geometrical thickness d_s and complex refractive index $\hat{n}_s(\lambda)=n_s(\lambda)-i\,\kappa_s(\lambda)$ are relatively simple, but those of {absorbing film/absorbing substrate} systems are elaborate, particularly $R(\lambda)$ formula [22-27]. In practice, laboratory fabricated films are not ideal in the sense they are not homogeneous and suffer from surface roughness, interfacial layers and inhomogeneity (in composition and thickness non-uniformity), which are governed by the substrate quality, film thickness, deposition method, preparation conditions and post-growth treatment. This makes the $T(\lambda)$-/$R(\lambda)$-formulations for such non-ideal optical systems much more unwieldy and somewhat inadequate for a rigorous optical analysis.

A variety of conventional curve-fitting programs, numeric optimization and purely algebraic methods were employed to analyze $T_{\text{exp}}(\lambda)-\lambda$ or $R_{\text{exp}}(\lambda)-\lambda$ data of various {film/substrate} structures incorporating uniform or non-uniform absorbing films, each of which has its own reliability, curbs and difficulties in application [28-54]. Conventional curve-fitting iterative methods entail a prior knowledge of models that describe spectral dispersion of $n(\lambda)$ and $\kappa(\lambda)$ and require sophisticated software that should yield a global solution of the problem and not multi-local solutions, which all give remarkable curve fits with diverse output results, most of which are unreliable or physically meaningless. The former requirement is difficult to accomplish for certain, while the latter is not always at hand and very expensive [28-31, 38, 42]. Nevertheless, conventional data curve-fitting is demandable and inevitable, particularly in case of complex, multi-layered structures of different optical properties.

Alternatively, a numeric optimization (so-called PUMA) method can be used to analyze $R_{\text{exp}}(\lambda)-\lambda$ data [32] or $T_{\text{exp}}(\lambda)-\lambda$ data [33-35] of air-supported {uniform absorbing film/transparent substrate} structures to determine $n(\lambda)$ and $\kappa(\lambda)$ of the film with no requisite of spectral dispersion relations in advance. The algebraic Swanepoel's envelope method (EM) of uniform films [36] is often employed to analyze $T_{\text{exp}}(\lambda)-\lambda$ spectra of such structures [37] also with no prior need to $n(\lambda)$ and $\kappa(\lambda)$ dispersion relations; but it is solely limited to $T_{\mathrm{exp}}(\lambda)-\lambda$ spectra that display many interference-fringe maxima and minima and exhibit wide portion of optically transparent region close to the substrate transmission, which are ideal systems that are not always realized in practice. A variety of modifications were reported in literature to include film inhomogeneity and substrate optical properties (absorption/dispersion) to improve analysis of $T_{\mathrm{exp}}(\lambda)-\lambda$ or $R_{\mathrm{exp}}(\lambda)-\lambda$ spectra of non-ideal air-supported {film/substrate} systems using Swanepoel's envelope methods (EMs) of uniform or non-uniform films [28, 38-54].

Normal-incidence transmission can be easily measured to a greater accuracy by most spectrophotometers covering ultraviolet (UV), visible (Vis) and near infrared (NIR) spectral regions compared to measurements of non-zero angle reflection that require calibration procedures using high-quality reference mirrors [29], besides involving analysis of more unwieldy $R(\lambda)$-formulae [22-27, 50, 51]. Thus, we shall here deal only with normal-incidence transmission of air-supported {non-uniform absorbing film/slightly-absorbing substrate} systems and with formulations required for analyzing their normal-incidence $T_{\mathrm{exp}}(\lambda)-\lambda$ spectra on the basis of Swanepoel EM of non-uniform films [28, 38-45, 52-54] using the approach of Richards et al. [42, 43]. This EM analytical approach proves to be conceivable for non-uniform films that are significantly absorbing over the whole wavelength range of interest and whose $T_{\mathrm{exp}}(\lambda)-\lambda$ spectra do not exhibit a transparent region at the high-λ side [17, 31, 42, 43, 48, 49, 54], which is viable in analysis of non-uniform films using procedures of original Swanepoel's EM when $T_{\mathrm{M}}(\lambda)\approx T_{\mathrm{S}}(\lambda)$ [39-41, 44-47, 52, 53].

Furthermore, there is significant variety in the reported optical constants of PbI_2 films prepared by various deposition routes and in their retrieved values of bandgap energy E_{g}, which are scattered in the range 2.1-2.6 eV [8-21, 31]. These diversities can be linked to the use of different film thicknesses, preparation conditions, optical characterization techniques and to the use of diverse/simple analytical approaches that sometimes exploited irrational/meek theoretical formulations for analyzing the measured optical data, besides implementing unalike models to typify the dispersion and absorption phenomena in studied lead iodide films.

To get further insight into some of unsettled issues of optical properties of PbI_2 films and features of their optical transmission, the normal-incidence $T_{\mathrm{exp}}(\lambda)-\lambda$ spectra of undoped flash-evaporated PbI_2 films on glass slides held at 200 °C were measured at room temperature (RT) in the range 400-900 nm and analyzed on the basis of Swanepoel EM of non-uniform films [39] using an extended approach reported by Richards et al. [42, 43]. This type of optical analysis has not yet been used to retrieve $n(\lambda)$ and $\kappa(\lambda)$ of PbI_2 films, a study that will shed more light on the spectral dispersion and electronic transition phenomena operative in lead iodide substance.

Experimental Details

A couple of physically and chemically pre-cleaned and heat-treated 1.1 mm thick microscopic glass slides were installed inside the bell-jar chamber of a Leybold coating's system, pumped down to less than 10^{-5} mbar base pressure. These slides were mounted tightly underneath a home-designed/constructed sample holder made of a massive copper (Cu) block, equipped with a thermocouple and cylindrical-shaped heater, energized from an electric heating/controller kit outside the chamber [17]. The slides were first heated to the required temperature (200 °C), which was controlled and kept steady there within ± 1 °C for several hours.

Undoped lead iodide films were deposited onto such pre-heated slides using a home-made flash-evaporation unit described elsewhere [17, 18]. This piece of apparatus is composed of an electrically-energized trigger system and a container filled in prior with finely-grinded lead iodide powder, which can be fed in tiny amounts through a perforated sieve into a long stainless steel (SS) tube that extends down close above a box-shaped molybdenum (Mo) crucible connected to two massive Cu electrodes [17, 18]. The Mo-crucible is first electrically heated to around 600 °C, held constant within $\pm$ 2 °C for several hours. The thickness d of deposited film was monitored and recorded by a quartz-crystal unit during evaporation at a low rate (1 nm/s) until the required final thickness was reached. The evaporation process was then stopped and the samples (film/substrate) were left to cool down in vacuum to RT. The final recorded d values of obtained flash-evaporated lead iodide films were 1 μm and 1.2 μm.

The structure and surface morphology of obtained flash-evaporated undoped lead iodide films were examined by conventional x-ray diffraction (XRD) and scanning electron microscopy (SEM), while electron dispersive spectroscopy (EDS) was used to determine their compositions. The flash-evaporated lead iodide films deposited on glass substrates sustained at 200 °C were found to be highly stoichiometric ($PbI_{1.9}$) and of a 2H-polytype hexagonal crystal structure [8, 16], with preferential crystalline orientation along the c-axis normal to the substrate surface [17, 18, 30]. Microscopic visualization showed that flash-evaporated PbI_2 films deposited on glass slides held at stable temperatures in the range $150-200\ ^{\circ}\mathrm{C}$ were pinhole-/crack-free and having virtuous smooth surfaces with hexagonal-shaped grains [17, 18, 30].

Room-temperature transmittance $T_s(\lambda)$ of a 1.1 mm thick microscopic glass slide and transmittance $T_{\exp}(\lambda)$ of the 1 μm and 1.2 μm thick undoped flash-evaporated PbI_2 films deposited on identical glass slides were measured as a function of the wavelength λ of light in the range 400-900 nm. Transmittance measurements were taken using a double-beam UV-Vis-NIR spectrophotometer (Varian Carry 100) at a scan rate of 120 nm/min and at 0.5 nm intervals, with the light beam being normally incident on surface of bare glass-slide and on the film surface of the {film/substrate} sample. Measurements of sample transmittance were made relative to corrected air-baseline transmission normalized to 100%, made first with both of the sample and the reference paths were open. The sample's transmittance was then measured with the sample being mounted vertically at its spectrophotometer entrance place along the path of its light beam, leaving the entrance of the reference light beam path uncovered.

Spectrophotometric transmission measurements are often affected by the sizes/widths of its slits and by natural line width of emerging light beam hitting the sample, the collective effect of which is embodied in spectrophotometer spectral band width (SBW) [36]. Thus, the choice of an SBW value is crucial to attain "uninfluenced" and accurately measurable transmission of studied sample. In this work, a 2 nm SBW was adopted in measurements of normal-incidence transmittance of air-supported {flash-evaporated PbI_2 film/glass slide} structures to ensure good signal-to-noise ratio of detected light and to reduce slit-size effect on transmission spectra [36]. Elimination of SBW effect on measured transmission can be made using Swanepoel procedure [36], but was found to be insignificant for experimental transmittance-wavelength ($T_{\exp}(\lambda)-\lambda$) spectra of our samples.

Results and Discussion

Measured Normal-Incidence Transmission-Wavelength Curves

Fig. 1 displays normal-incidence $T_{\exp}(\lambda)-\lambda$ spectra of (PbI_2 film/glass-slide) samples F1 and F2 of the 1 μm and 1.2 μm thick flash-evaporated PbI_2 films, respectively, as well as the $T_s(\lambda)-\lambda$ spectrum of a typical free-standing 1.1 mm thick bare glass slide, in the wavelength-range 400-900 nm. Several interesting features of these measured normal-incidence transmission spectra are worth discussing, as they provoke optical analysis of such spectra (to be carried out in later sections).

It is noted that the substrate transmittance is almost flat, with nearly constant $T_s(\lambda)$-values ranging from 89% to 91% in the λ-range covering the entire transmission and absorption regions of {PbI_2 film/substrate} samples. Figure 1 shows that the $T_{\exp}(\lambda)-\lambda$ curves of both {PbI_2 film/substrate} samples exhibit in the λ-range 520-900 nm several well-separated interference-fringe maxima and minima, the number of which increases and their spectral width becomes narrower with increasing film thickness. The presence of numerous well-resolved interference-fringe maxima and minima on experimental transmission curves of air-supported {film/substrate} structures facilitates the workability and accuracy of their optical analysis on the basis of Swanepoel EMs [36-42].

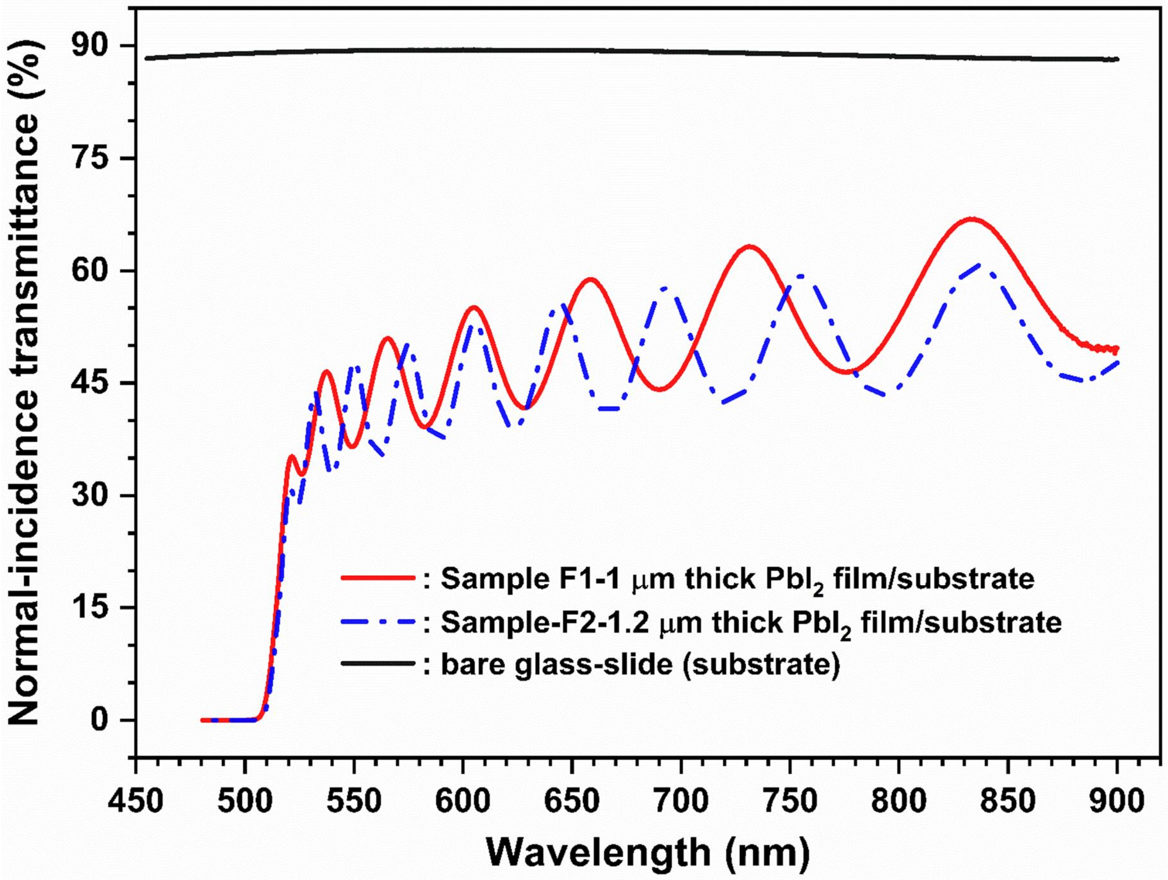

FIG. 1. Wavelength dependency of measured room temperature normal-incidence transmittances of a typical bare glass slide and of samples F1 and F2 which are air-supported {1 μm/1.2 μm thick flash-evaporated PbI_2 films/glass-slide (at 200 °C)} structures.

Below $\lambda \sim 520$ nm, the $T_{\text{exp}}(\lambda) - \lambda$ curves of both optical structures start to fall down steeply over a narrow λ-range towards zero transmission that initiates at $\lambda \sim 505$ nm. This abrupt decline in the $T_{\text{exp}}(\lambda) - \lambda$ curves of studied samples is merely due to light absorption in the flash-evaporated PbI_2 films themselves. An abrupt optical absorption trend is a characteristic of crystalline materials, which commonly have a vertically sharp fundamental optical absorption edge, with minor bandgap-tailing often encountered in amorphous material films [56-58]. These results are in good accord with the measured XRD patterns of flash-evaporated PbI_2 films that possess highly hexagonal 2H-polytyptic structure [17, 18, 30].

Nevertheless, there are some features in the $T_{\text{exp}}(\lambda) - \lambda$ spectra of {PbI_2 film/substrate} samples of Fig. 1 that render their analysis rather challenging. Such transmission curves show that the maxima $T_{\text{M}}(\lambda)$ of their interference-fringe patterns are much lower than $T_{\text{s}}(\lambda)$ in the studied λ-range, with a depression $\Delta T(\lambda) = T_{\text{s}}(\lambda) - T_{\text{M}}(\lambda)$ ranging between 55% at $\lambda \sim 525$ nm and 25% at $\lambda \sim 835$ nm for sample F1 of 1 μm thick PbI_2 film, and much larger for that of sample F2 of the 1.2 μm thick PbI_2 film. This implies that these transmittance spectra do not exhibit at the high-λ side any optical transparent region, the existence of which is useful for applying the procedures of traditional Swanepoel's EMs of uniform and non-uniform films to some optical systems [36, 37, 39, 44-47, 52, 53].

Optical Analysis of $T_{\text{exp}}(\lambda) - \lambda$ Spectra of {Air/Flash-evaporated PbI_2 Film/Glass-Slide/Air} Structures

The diminishing of normal-incidence transmittance and its interference-fringe maxima of our {PbI_2 film/glass-slide} samples F1 and F2 can then be related to true optical absorption in the film itself and to other causes of different origins. The former cause is undoubtedly the leading term in the strong optical absorption region that becomes more operative with progressive decrease in wavelength towards the fundamental absorption edge of the substance; however, optical absorption cannot be exclusively responsible for observed drastic transmittance decrease in the weak and intermediate optical absorption regions of studied {PbI_2 film/glass-slide} samples F1 and F2. Studies on many {film/substrate} systems suggested that diminution in the weak and medium absorption region of transmission spectra can be related to interference-fringe shrinking due to spectral bandwidth (SBW) [36], inhomogeneity in the film refractive index (Δn) and its thickness non-uniformity (Δd) [36, 38-49], absorption in substrate [38, 42, 43, 48, 49] and light scattering from surface bumpiness [25]. The latter is an unwieldy issue to treat and was tolerated here as visual inspection of our stoichiometric PbI_2 films revealed good surface smoothness and their SEM patterns showed no surface cracks/pinholes, but close-tight hexagonal structure grains [17, 18, 31]. Here, we shall explore the effect of these causes on the measured $T_{\mathrm{exp}}(\lambda)-\lambda$ spectra of our samples F1 and F2 in some detail.

Large widths of the spectrophotometer slits, effected *via* SBW, often cause shrinkage of the interference-fringe maxima and minima and should be corrected for to achieve accurate optical analysis of transmission spectra of films (uniform or non-uniform) [36, 39, 42]. A large width of spectrometer slit affects significantly and erroneously the determined thickness of the film and its refractive index in the region that is crowded in maxima/minima peaks with small spectral widths and separations [36]. Before starting analysis of the $T_{\mathrm{exp}}(\lambda)-\lambda$ spectra of our samples by the analytical approach of Richards et al. [42, 43], we carried out slit-width correction to measured $T_{\mathrm{M}}(\lambda_{\mathrm{tang}})/T_{\mathrm{m}}(\lambda_{\mathrm{tang}})$ using the procedure of Swanepoel [36] (cf. Eq. (A.14) and Eq. (A.15) in supplementary material). But, the 2 nm SBW chosen in the present work was found to be conceivable for minimizing possible slit-width induced influence on such measured maxima and minima, with negligible SBW-corrections to their magnitudes.

Substrate absorption alters the magnitude of measured transmission maxima/minima of films deposited on weakly-absorbed substrates [38, 40-49]. Close inspection of $T_{\mathrm{s}}(\lambda)-\lambda$ spectrum of Fig. 1 reveals minor absorption inside the 1.1 mm thick glass slide in the range 400-900 nm and marginally affects $T_{\mathrm{exp}}(\lambda)-\lambda$ spectra of Fig. 1 if divided, to a first approximation [38, 42], at each λ by $x_{\mathrm{s}}(\lambda)=\exp(-\alpha_{\mathrm{s}}(\lambda)d_{\mathrm{s}})$ [42, 43]. This term is solely originating from the absorption of primary light beam passing through the substrate, as the contribution of all internally reflected beams inside it is trivial in its weak absorption region. So, correction for substrate absorption was abandoned in our analysis, supported by the results of a thorough curve-fitting of the $T_{\mathrm{s}}(\lambda)-\lambda$ data of Fig. 1 [30, 31]. Yet, instead of using a constant $n_{\mathrm{s}}(\lambda)$ [36, 37, 39], we fitted part (in the λ-range 400-900 nm) of the $n_{\mathrm{s}}(\lambda)-\lambda$ data obtained from such curve-fitting analysis to a 5-constant Cauchy dispersion relation of the form:

$$n_{\mathrm{s}}(\lambda)=A_0+\frac{A_2}{\lambda^2}+\frac{A_4}{\lambda^4}+\frac{A_6}{\lambda^6}+\frac{A_8}{\lambda^8} \qquad (1)$$

where A_0, A_2, A_4, … etc. are constants that were determined from the curve fit. The obtained fit equation was exploited to find directly $n_{\mathrm{s}}(\lambda_{\mathrm{M}}/\lambda_{\mathrm{m}})$ at any wavelength of the measured maxima/minima of studied air-supported {PbI_2 film/glass-slide} samples F1 and F2. The results of $n_{\mathrm{s}}(\lambda)-\lambda$ data and its fit curve are as shown in Fig. 2.

Further, a lateral variation in the refractive index Δn of a uniformly thick film of thickness d and an average refractive index $\bar{n}$ can be modelled in a similar way to that adopted for a lateral thickness variation Δd of a non-uniform film of an average thickness $\bar{d}$ and refractive index n [39]. Both non-uniformities compress the interference fringes maxima and minima and their formulations in Δn and Δd are similar, as $\Delta n\, d \equiv n\, \Delta d$ [39]. Thus, it is practically difficult to determine whether Δn or Δd is causing the shrinking of transmission spectra, even if SBW-effect is the same with no variation in n along the film depth [39, 42, 43]. So, we here have adopted only the effect of thickness non-uniformity, besides the effect of optical absorption in the film, to treat measured $T_{\mathrm{exp}}(\lambda)-\lambda$ spectra of Fig.1 on the basis of Swanepoel EM of non-uniform films using the analytical procedures of Richards et al. [42, 43].

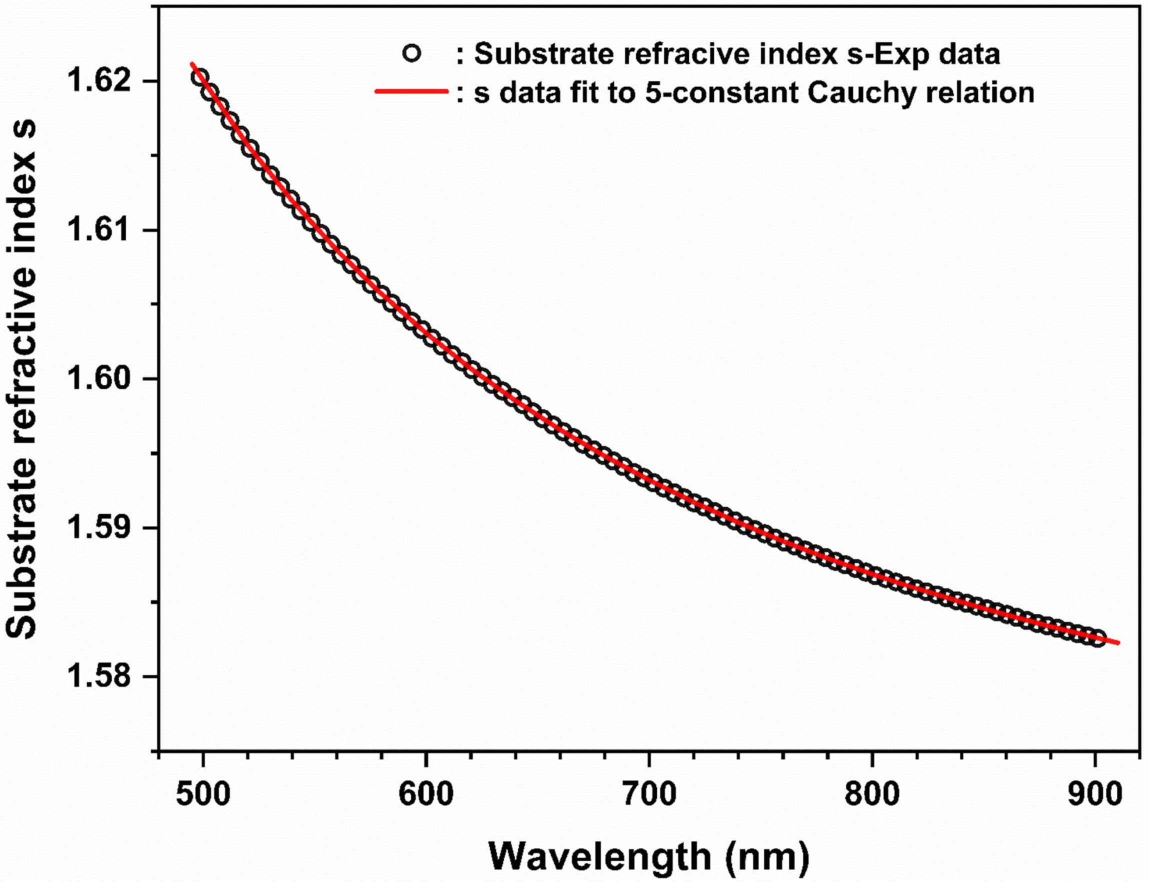

FIG. 2. Data (open circles) of index of refraction s as a function of wavelength λ for a typical glass slide similar to those used as substrates for studied flash-evaporated lead iodide films. The solid curve represents a curve fit of this data to the 5-constant Cauchy dispersion equation described in Eq. (1).

The Basic Formulations of Swanepoel Envelope Method (EM) of Non-Uniform Films

Optical analysis presented in supplementary material is exclusively based on Swanepoel's envelope theory of non-uniform films [39] and is limited for transmission spectra exhibiting transparent region at the high-λ side. It is assumed that $T_{\mathrm{M}}(\lambda) \approx T_s(\lambda)$ to find Δd and $n(\lambda)$ in this transparent region and in the weak and medium absorption regions, besides adopting the formulae relating the measured T_{M} and T_{m} of non-uniform films to T_{M0} and T_{m0} of uniform films of same material and thickness $d = \bar{d}$, the average thickness of non-uniform film [39, 44-47, 52, 53].

The measured transmittance $T_{\Delta d}(\lambda)$ of a non-uniform film of refractive index $n(\lambda)$, average thickness $\bar{d}$ and thickness non-uniformity Δd ($\ll \bar{d}$) on a transparent/weakly-absorbing substrate can be approximately described in the range $0 < \Delta d < \lambda/4\,n(\lambda)$ by an expression of the form (Appendix A in supplementary material) [38-45]:

$$T_{\Delta d} = \frac{1}{d_{\max} - d_{\min}} \times \int_{d_{\min}}^{d_{\max}} \frac{A \exp[-\alpha(\lambda)\bar{d}]}{\left(B - C \cos\left[\frac{4\pi n(\lambda) d'}{\lambda}\right] \exp[-\alpha(\lambda)\bar{d}] + D \exp[-2\alpha(\lambda)\bar{d}]\right)} \times \mathrm{d}d' \qquad (2)$$

where $d_{\min} = \bar{d} - \Delta d$ and $d_{\max} = \bar{d} + \Delta d$, while the constants A, B, C and D are given by the relations below [36]:

$$A = 16 n_s n^2, B = (n+1)^3 (n + n_s^2),$$
$$C = 2(n^2 - 1)(n^2 - n_s^2),$$
$$D = (n-1)^3 (n - n_s^2). \qquad (3)$$

As discussed in some detail in Appendix A of supplementary material, the measured/calculated maxima $T_{\mathrm{M}\Delta d,x}(\lambda_{\mathrm{M}}/\lambda_{\mathrm{m}})$ and minima

$T_{\mathrm{m}\Delta d,x}(\lambda_{\mathrm{m}}/\lambda_{\mathrm{M}})$ of a non-uniform film of refractive index $n(\lambda)$, absorption coefficient $\alpha(\lambda)$, average thickness $\bar{d}$, absorbing parameter $\bar{x}(\lambda) = \exp\left[-\alpha(\lambda)\bar{d}\right]$ and thickness non-uniformity Δd can be shown to be described by the following formulae [39-45]:

$$T_{\mathrm{M}\Delta d,x} \approx \left(\frac{\lambda}{2\pi n\Delta d}\right)\frac{a_x}{\sqrt{1-b_x^2}}\tan^{-1}\left[\frac{1+b_x}{\sqrt{1-b_x^2}}\tan\left(\frac{2\pi n\Delta d)}{\lambda}\right)\right] \quad (4)$$

$$T_{\mathrm{m}\Delta d,x} \approx \left(\frac{\lambda}{2\pi n\Delta d}\right)\frac{a_x}{\sqrt{1-b_x^2}}\tan^{-1}\left[\frac{1-b_x}{\sqrt{1-b_x^2}}\tan\left(\frac{2\pi n\Delta d)}{\lambda}\right)\right]. \quad (5)$$

The parameters a_x and b_x are given by the relations below:

$$a_x = \frac{A\bar{x}}{B + D\bar{x}^2} \text{ and } b_x = \frac{C\bar{x}}{B + D\bar{x}^2}\,. \quad (6)$$

Eqs. (4) and (5), combined with Eq. (6), are valid for both transparent region ($\bar{x} = 1$) and weak and medium absorption regions ($\bar{x} < 1$) of transmission spectra of air-supported {non-uniform film/substrate) structures and are independent transcendental equations that can be solved simultaneously to get a unique solution of their two unknowns. They form the basic expressions on which algebraic analysis of transmission spectra of such structures in these optical absorption regions by the conventional Swanepoel EM of non-uniform films is exclusively based to evaluate Δd, $\bar{d}$ and $n(\lambda)$ of the film under consideration once the values of maxima $T_{\mathrm{M}}(\lambda_{\mathrm{M}}/\lambda_{\mathrm{m}})$ and minima $T_{\mathrm{m}}(\lambda_{\mathrm{m}}/\lambda_{\mathrm{M}})$ are obtainable, combined with the corresponding values of $n_{\mathrm{s}}(\lambda_{\mathrm{M}}/\lambda_{\mathrm{m}})$. In the present analysis, the latter can be found from Fig. 2 and its numerical fit relation (Eq. (1)). Eventually, $\alpha(\lambda)$ and bandgap energy E_{g} of the film sample can then be determined once the respective values of $\bar{x}(\lambda)$ are appropriately determined [39-45].

Procedure for Constructing Transmission Interference-Fringe Maxima and Minima Envelope Curves

It is clear that the first step to proceed with the above-described optical analysis is to determine accurately the values of interference-fringe transmission maxima $T_{\mathrm{M}}(\lambda_{\mathrm{M}}/\lambda_{\mathrm{m}})$ and minima $T_{\mathrm{m}}(\lambda_{\mathrm{m}}/\lambda_{\mathrm{M}})$ at the corresponding tangent wavelengths λ_{M} and λ_{m}, which were here accomplished using the source package ENVELOPE computer program of McClain *et al.* [55] (http://dlmf.nist.gov). The McClain ENVELOPE program usually finds the measured $T_{\mathrm{M}}(\lambda_{\mathrm{M}})$ and minima $T_{\mathrm{m}}(\lambda_{\mathrm{m}})$ and then constructs continuous, monotonic $T_{\mathrm{M}}(\lambda_{\mathrm{M}}/\lambda_{\mathrm{m}})$ and $T_{\mathrm{m}}(\lambda_{\mathrm{m}}/\lambda_{\mathrm{M}})$ envelope curves, which are bound and tangent to these transmission maxima and minima.

This ENVELOPE program was applied to maxima and minima of transmission spectra of our samples few times *via* decreasing progressively the tolerance of computation to get optimal numerals of T_{M} and T_{m} and their λ_{M} and λ_{m}. The section of code in the original ENVELOPE program where each pair of transmission maxima and minima data (x, y) is replaced by the average of itself and its two nearest neighbor points was commented out as done by Richards *et al.* [42, 43]. This is justified by low noise in our $T_{\mathrm{exp}}(\lambda)$ data, a valuable aspect for smoothing envelope curves and using $T_{\mathrm{exp}}(\lambda) > 0.1\%$ to avoid noisy (due to fluctuations in detected signal) data points from being treated by ENVELOPE algorithm as extrema. A second modification in this program was increasing the dimension of the array to improve final smoothing [42, 43] before ENVELOPE code was re-compiled.

The ENVELOPE program starts by an initial smoothing process using a "piecewise cubic polynomial" fit to the experimental data points and a second smoothing when a first estimate of the tangent points is achieved. Several trials of tolerance factors were performed. The ENVELOPE calculations converge and highly acceptable fitted envelope curves were obtained when the values 0.04 and 0.003 of tolerance factors were used for the initial and final smoothing process. Using the new smoothed data, the program then attempts to find estimates for the tangent points where the envelope curves will touch the data curve. This is done by locating intervals where smoothed data curve is either concave or convex, with the tangent points for top envelope were initialized to be the midpoints of each concave interval, while those for bottom envelope were set at the midpoints of each convex interval. The first or last data point is excluded from the last smoothing process. These points were used only if they represent a local maximum or minimum and in this case, the tangent point estimate was taken to be the local maximum or minimum point rather than the midpoint of the interval.

The true tangent point for an endpoint interval may lie outside the range of the original data points and the ENVELOPE algorithm will not converge correctly. If the endpoint interval contains a local maximum or minimum, the true tangent point is guaranteed to lie nearby and the algorithm will then converge properly. The output of the ENVELOPE consists of two files: one is the number of tangent points having been found for each envelope and the coordinates of each "top" and "bottom" extrema in the oscillating data. The second file contains the smoothed data for both the top and bottom curves. It is worth noting here that no visible improvement of the resulting top and bottom tangent points was noticed upon performing the second modification. Nevertheless, this minor modification was kept in the executable version. The data file containing the finally determined values of $T_{\mathrm{M}}(\lambda_{\mathrm{M}}/\lambda_{\mathrm{m}})$ and $T_{\mathrm{m}}(\lambda_{\mathrm{m}}/\lambda_{\mathrm{M}})$ is stored and kept for use in the required optical analysis. An example of such ENVELOPE points corresponding to interference-fringe maxima and minima of measured transmission spectra of samples F1 and F2 of the 1 μm and 1.2 μm thick flash-evaporated PbI_2 films, respectively, is shown in Fig. 3.

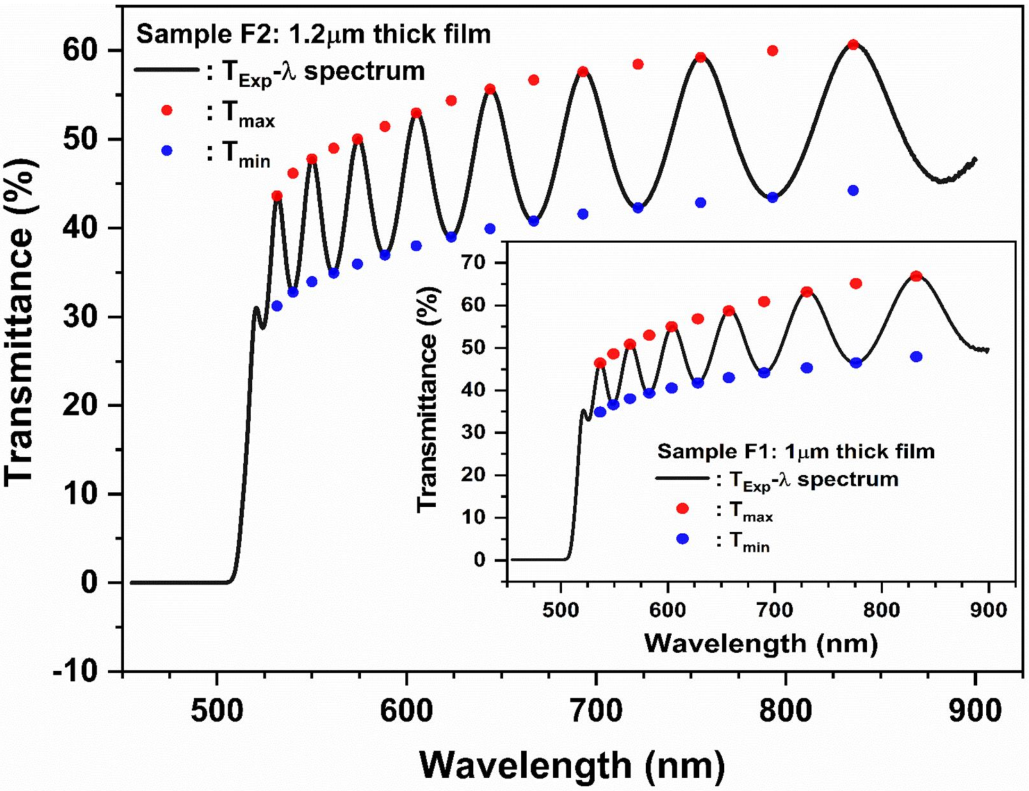

FIG. 3. The interference-fringe maxima and minima points of measured transmission spectra of samples F1 and F2 of the 1 μm and 1.2 μm thick flash-evaporated PbI_2 films, respectively, as determined from ENVELOPE program of McClain et al. [55].

Determination of PbI_2 Film Optical Constants Using the Extended Swanepoel EM of Non-Uniform Films

The thickness non-uniformity Δd and $n(\lambda)$ of the non-uniform film are usually evaluated by solving simultaneously the two transcendental equations given in Eq. (4) and Eq. (5) with $\bar{x} = 1$ being inserted in Eq. (6) using the measured/calculated maxima $T_{\mathrm{M}}(\lambda_{\mathrm{M}}/\lambda_{\mathrm{m}})$ and minima $T_{\mathrm{m}}(\lambda_{\mathrm{m}}/\lambda_{\mathrm{M}})$ [39-41]. However, the calculated values of Δd are often drastically varying with wavelength, so a feasible Δd-value had to be chosen for use in the calculations of $n(\lambda)$ and $\alpha(\lambda)$ in the weak and medium ($\bar{x} < 1$) region. In many studies based on Swanepoel EM of non-uniform films [39], this was often made by selecting arbitrarily/luckily few of the calculated Δd-values and taking their average to be that optimum value of Δd.

Further, some {non-uniform film/substrate} samples do not exhibit a transparent region and are absorbing in the whole wavelength range [42, 43, 48, 49, 54], as is also seen from Fig. 1. Assuming $T_{\mathrm{M}} \approx T_{\mathrm{s}}$ for such transmission spectra for use in the formulae relating T_{M} and T_{m} of a non-uniform film to T_{M0} and T_{m0} of a uniform one with $d = \bar{d}$ [39, 44-47, 52, 53] or picking a capricious Δd-value [39-41, 54] sometimes yield irrational results and is questionable. An extended version of Swanepoel's EM of non-uniform films has been suggested by Richards et al. [42, 43] for treating transmission spectra of non-uniform films that are absorbing even at high-λ side *via* choosing an initial value for Δd and varying it till a coincidence between the calculated (simulated) and measured transmission curves is obtained. This approach is adopted to analyze $T_{\exp}(\lambda) - \lambda$ spectra of Fig. 1. As discussed above, however, no correction was made to these $T_{\exp}(\lambda)$ spectra at each λ or to respective $T_{\mathrm{M}}(\lambda_{\mathrm{M}}/\lambda_{\mathrm{m}})$ and $T_{\mathrm{m}}(\lambda_{\mathrm{m}}/\lambda_{\mathrm{M}})$ at each λ_{M} and λ_{m} for slit-width effect or absorption in the substrate. Our analysis only includes the substrate dispersive $s\,(\lambda_{\mathrm{M}}/\lambda_{\mathrm{m}})$-values in the formulae containing $T_{\mathrm{M}}(\lambda_{\mathrm{M}}/\lambda_{\mathrm{m}})$ and $T_{\mathrm{m}}(\lambda_{\mathrm{m}}/\lambda_{\mathrm{M}})$, as done by Richards et al. [42, 43]. This was not used by Swanepoel [39], but is also adopted in other studies using procedures of conventional Swanepoel's EM of non-uniform films [38, 40-49, 52-54].

Lastly, we applied the approach of Richards et al. [42, 43] to analyze the $T_{\mathrm{M}}(\lambda_{\mathrm{M}}/\lambda_{\mathrm{m}})$ and $T_{\mathrm{m}}(\lambda_{\mathrm{m}}/\lambda_{\mathrm{M}})$ to calculate Δd at each λ_{M} and λ_{m}, the value of which was varied until the calculated values of Δd, $n(\lambda)$, $\alpha(\lambda)$ and $\bar{d}$ of studied flash-evaporated PbI$_2$ films re-generated their respective measured transmission curves. The finally-approved $n(\lambda) - \lambda$ and $\alpha(\lambda) - \lambda$ data was then used to elucidate the spectral dispersion and electronic transitions operating in these undoped flash-evaporated PbI$_2$ films.

All of the implemented procedures and the algebraic calculation stages of this extended version of Swanepoel EM of non-uniform films have been integrated in a compact computational program written in Mathematica. Before executing the entire program in a single run, all of its individual steps were first checked in sequence for their workability and correctness.

Determination of the Thickness Variation Δd for the Non-uniform Flash-Evaporated PbI$_2$ Films

Thickness non-uniformity Δd of a film and its optical absorption affect dissimilarly its transmission spectrum, in the sense that an increase in Δd shrinks the interference-fringe minima and maxima at all wavelengths, while an increase in film absorption coefficient $\alpha(\lambda)$ reduces progressively the magnitude of both maxima and minima fringes (it reduces the geometric mean of transmission spectrum) [39, 43]. In this analysis, we assumed that the observed transmission interference-fringe pattern of our samples F1 and F2 is related to non-uniformity in the thickness of the PbI$_2$ film itself and the film is also optically absorbing over the whole wavelength range studied.

To complete analyzing transmission spectra of the non-uniform, absorbing PbI$_2$ films shown in Fig. 1, where no transparent region can be seen, on the basis of Swanepoel EM of non-uniform films, it is indispensable to determine first an accurate value for their thickness non-uniformity Δd. Put $\bar{x} = 1$ in the coefficients a_x and b_x given in Eq. (6) and insert their coefficients $A, B, C\ and\ D$ defined in Eq. (3) in Eq. (4) and Eq. (5) to reduce them to two independent transcendental equations in Δd and n only, as substrate's refractive index n_s is already known.

Now, the measured/calculated values of $T_{\mathrm{M}}(\lambda_{\max}/\lambda_{\min})$ and $T_{\mathrm{m}}(\lambda_{\min}/\lambda_{\max})$ were inserted into them, which were solved simultaneously to find the two unknowns Δd and $n(\lambda_{\mathrm{tang}})$ at each tangent wavelength λ_{tang} ($= \lambda_{\max}$ and $\lambda_{\min}$) using the rigorous Mathematica 'FindRoot package". At this computational stage, the optical absorption in the film is ignored and the obtained values of $n(\lambda_{\mathrm{tang}})$ are usually overlooked, as the purpose here is exclusively to determine a value for Δd, which should be a λ-independent inherent constant film quantity. However, the values of Δd calculated by this tactic usually show drastic variation with λ [38-43, 54], so selecting an acceptable value for Δd becomes a challenging issue and is crucial for subsequent procedures used to determine optical constants of the film in weak, medium and strong absorption regions.

Adopting an average of the whole/part of the obtained Δd-values and/or a lucky/arbitrary choice of a Δd-value [39-41, 54] is not a good methodology for determining an accurate value for this parameter; thus, finding a more reliable value for Δd turns out to be tricky. A rational value for Δd might be inferred from a plot of $\Delta d(\lambda_{\text{tang}})$-Vs-$\lambda_{\text{tang}}$ and picking a reminiscent value of Δd if a saddle-like portion exists on such a plot in the medium absorption region [38]. If the film transmission exhibits a transparent region at high-λ side, then Δd might be the asymptotic value at such high wavelengths [42]. However, if the film is absorbing over the whole transmission spectrum with no transparent region, as displayed in Fig. 1, and if no real asymptotic Δd value or saddle-like part on $\Delta d(\lambda_{\text{tang}})$-$Vs$-$\lambda_{\text{tang}}$ plot can be adopted, as for our PbI$_2$ films, the Δd values of which calculated from simultaneous solution of Eq. (4) and Eq. (5) with $\bar{x} = 1$ are depicted in Fig. 4, the situation becomes more problematic. Richards et al. [42, 43] suggested that even choosing a Δd-value from asymptotic regime should be used as an initial guess for succeeding calculations underlying the optical analysis based on Swanepoel's EM of non-uniform films that are optically absorbing over the entire wavelength range of interest. In the absence of both asymptotic-type or saddle-like Δd region, such initial Δd can be selected from calculated Δd values scattered in medium absorption region [38].

An incorrect attribution of actual optical absorption in the film to be due to the thickness variation that has dissimilar effect on the maxima and minima should be evident when the calculated values of optical constants and film thickness are used to regenerate the measured transmission spectrum. If the generated data does not lie correctly on the measured transmission curve, then the value of Δd has to be adjusted accordingly, most likely to lower values, until an optimum is acquired and a virtuous match between the measured and generated transmission data is realized. This method forms the basis of a checking procedure for the uniqueness solution of Eq. (4) and Eq. (5) that can be considered to be reliable, as there should be only one unique solution for them [39]. The procedures of this EM analytical approach and associated formulations are adopted to analyze measured normal-incidence $T_{\text{exp}}(\lambda) - \lambda$ spectra of our {PbI$_2$ film/substrate} samples.

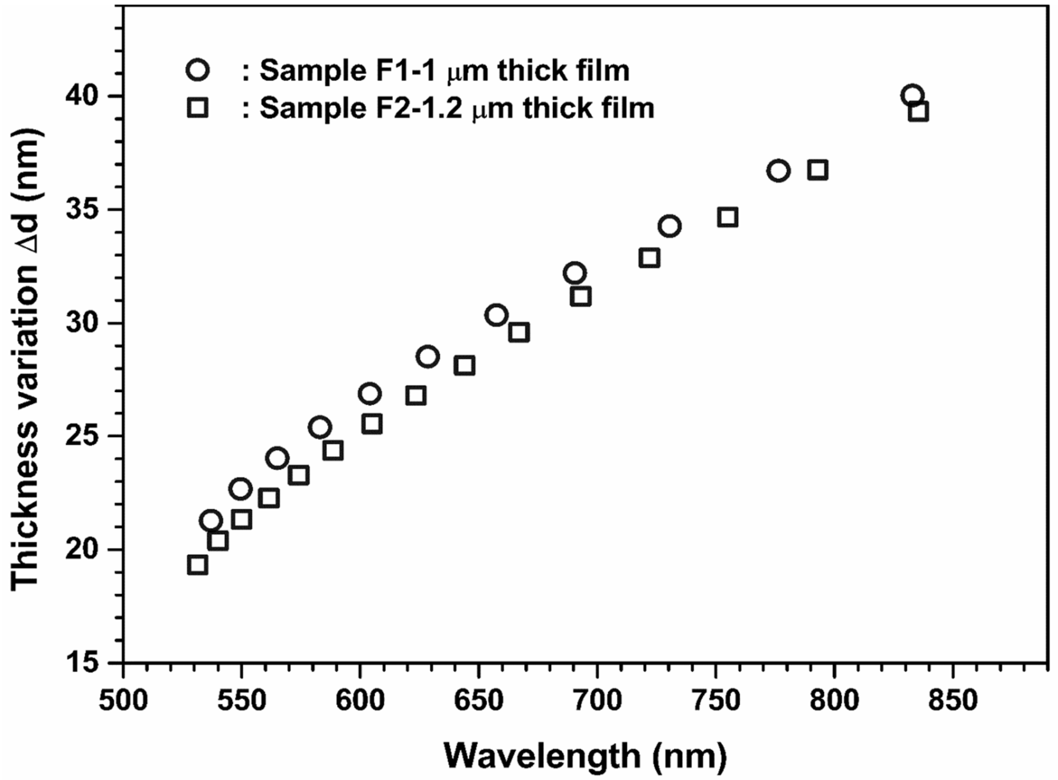

FIG. 4. Wavelength variation of thickness non-uniformity Δd calculated from simultaneous solution of the two transcendental formulae in Eq. (4) and Eq. (5), assuming $\bar{x} = 1$, for samples F1 and F2 of the 1 μm and 1.2 μm thick flash-evaporated PbI$_2$ films, respectively.

Determination of Film's Optical Constants and Average Thickness in Weak and Medium Absorption Regions

In principle, having a reasonable value for Δd, Eq. (4) and Eq. (5) can then be solved simultaneously, this time to find the two unknowns $n(\lambda_{\text{tang}})$ and $\bar{x}(\lambda_{\text{tang}})$ at each extreme wavelength λ_{tang} (= $\lambda_{\max}$ and $\lambda_{\min}$) in the weak and medium absorption regions ($\bar{x} < 1$) using the absorbing coefficients a_{x} and b_{x} given in Eq. (6) with their A, B, C and D coefficients given in Eq. (3) that incorporate n and s, which is determined separately in advance. These expressions are another two independent transcendental equations that have one unique solution for $n(\lambda_{\text{tang}})$ and $\bar{x}(\lambda_{\text{tang}})$ at each $\lambda_{\max}$ or $\lambda_{\min}$ in the validity range $0 < \bar{x} \lessapprox 1$ [39].

The absorption coefficient $\alpha(\lambda_{\text{tang}})$ in the weak and medium absorption regions can be found from the determined $\bar{x}(\lambda_{\text{tang}})$ using the relation $\alpha(\lambda_{\text{tang}}) = -\ln \bar{x}(\lambda_{\text{tang}})/\bar{d}$, if we have at hand an accurate value for the film average thickness $\bar{d}$, which, however, is practically difficult to measure. In optical analysis based on Swanepoel's EM of non-uniform films, $\bar{d}$ can be found from the interference condition given by [39]:

$$2\bar{d}n(\lambda_{\text{tang}}) = m\lambda_{\text{tang}}. \tag{7}$$

This can be attained by using $n(\lambda_{\text{tang}})$ values at $\lambda_{\max}$ or $\lambda_{\min}$ of the nearest neighboring extrema [36, 39], with m being the interference order (integer for maxima and half-integer for minima displayed on measured transmission spectrum). However, a more feasible value of $\bar{d}$ can be attained by the use of the expression given below [39]:

$$\frac{\ell}{2} = 2\,\bar{d}\left[\frac{n(\lambda)}{\lambda}\right] - m_1, \tag{8}$$

where ℓ = 0, 1, 2, 3, 4, ……, with ℓ = 0 for the first observable extrema on the high-wavelength side, which corresponds to interference order m_1 that should be an integer for maxima and half-integer for minima.

A proper linear portion of a plot of $\ell/2$ against $n(\lambda_{\text{tang}})/\lambda_{\text{tang}}$ for $\ell = 0, 1, 2, 3, 4, \ldots$ can be fitted to Eq. (8), with its slope giving $2\bar{d}$ and its negative intercept is m_1, which should be then round off to the nearest integer/half-integer numeral m_0 for the first visible maxima/minima in the long-λ region. An improved value for $\bar{d}$ can then be found from a linear portion of a new $\ell/2 - n(\lambda_{\text{tang}})/\lambda_{\text{tang}}$ plot, with m_0 being now kept fixed and treated as a constant parameter in the fitting process on basis of Eq. (8). The straight line is normally a poor fit to the points if the wrong m_0 value is used; thus, unity (1) would sometimes be added or subtracted from the used m_0-value and the fit procedure has to be repeated.

The finally obtained values of $\bar{d}$ and m_0, with the interference-order m being increased progressively from m_0 by 1/2 for the maxima and minima at shorter λ_{tang}, are then fed back into Eq. (7) to determine more accurate values for $n(\lambda_{\text{tang}})$ at $\lambda_{\max}/\lambda_{\min}$ of the observed transmission interference-fringe pattern in the weak and medium absorption regions. Further, once an improved value of $\bar{d}$ is determined, the values of $\alpha(\lambda_{\text{tang}})$, hence $\kappa(\lambda_{\text{tang}}) = \alpha(\lambda_{\text{tang}})\lambda_{\text{tang}}/4\pi$, can be determined in weak and medium absorption regions using the determined $\bar{x}(\lambda_{\text{tang}})$.

Determination of Optical Constants of the Film in the Strong Optical Absorption Region

In the region of medium to nearby strong optical absorption, the interference fringes become rather small and experimental uncertainties in the magnitude of the last few resolved extrema often lead to erroneous calculated values of $\alpha(\lambda_{\text{tang}})$ [36, 39]. Hence, one has to choose only the number of data points, counted from the long-λ side, which do not produce randomly varying and noisy $\alpha(\lambda_{\text{tang}})$ values. Values of $\alpha(\lambda)$ at wavelengths of non-adopted last extrema in the medium absorption region and at shorter wavelengths in the strong absorption region cannot be determined by the use of interference condition given in Eq. (7), which is not strictly valid in the absorption region, and there is no means of extracting $n(\lambda)$ values from the interference-free transmission curve alone. The values of $\alpha(\lambda)$ in the quasi-/strong- optical absorption regions can be obtained by the use of different means [36, 37, 39-43].

A tactic to achieve such goal is to extrapolate the non-noisy $n(\lambda_{\text{tang}})$ of the weak and medium absorption regions in the remainder of the spectrum *via* fitting such $n(\lambda_{\mathrm{tang}}) - \lambda_{\mathrm{tang}}$ data to an appropriate dispersion formulation. The obtained fit $n(\lambda)$-formula can then be utilized to determine the respective values of $x(\lambda)$, and hence of $\alpha(\lambda)$, in the weak and medium absorption regions using an evocative formulation relating $n(\lambda)$ and $x(\lambda)$, which involves the transmission maxima T_{M} as that described by the expression given below [36, 40, 42-45]:

$$x = \frac{E_{\mathrm{M}} - [E_M^2 - (n^2-1)^3(n^2-n_s^4)]^{\frac{1}{2}}}{(n-1)^3(n-n_s^2)};$$

$$E_{\mathrm{M}} = \frac{8n^2 n_s}{T_{\mathrm{M}}} + (n^2-1)(n^2-n_s^2). \qquad (9)$$

Eq. 9 has been frequently used to determine $\alpha(\lambda)$ for films with uniform thickness in the weak and medium absorption regions since $n(\lambda)$ and $n_s(\lambda)$ are already known [36, 37]; nonetheless, it has been argued that Eq. 9 can also be valid for non-uniform films in the spectral region where the interference fringes start to disappear and thus the maxima and minima envelope curves converge to a single curve in the strong absorption region, in which $T_{\mathrm{M}} \approx T_{\mathrm{m}} \approx T$ [42-45]. Alternatively, a formula that includes interference-free transmission geometric mean $T_\alpha = \sqrt{T_{\mathrm{M}} T_{\mathrm{m}}}$ [36, 42, 43] can also be utilized to determine $x(\lambda)$ in weak, medium and strong absorption regions. This formula is often used in optical and infrared studies and is described in the expression given by [39]:

$$x = \frac{\left\{G - [G^2 - (n^2-1)^6(n^2-n_s^4)^2]^{\frac{1}{2}}\right\}^{\frac{1}{2}}}{(n-1)^3(n-n_s^2)},$$

$$G = \frac{128n^4 n_s^2}{T_\alpha^2} + n^2(n^2-1)^2(n_s^2-1)^2 + (n^2-1)^2\,(n^2-n_s^2)^2 \;. \qquad (10)$$

For spectral wavelengths shorter than where the last extrema is resolved, Eq. (9) and Eq. (10) can be used for calculating $x(\lambda)$, but with taking the transmission value incorporated into them directly from the original spectrum and using the extrapolated $n(\lambda)$ values [40-45]. In the present study, Eq. (10) has been found to yield more satisfactory results for the transmission spectrum of our non-uniform undoped flash-evaporated $\mathrm{PbI_2}$ films.

The above-described comprehensive optical analytical procedures based on Swanepoel's EM of non-uniform films [39] and extended to deal with transmission spectra of films that are absorbing in the whole λ-range of interest [42, 43] complete the determination of the optical constants $n(\lambda)$, $\alpha(\lambda)$ and $\kappa(\lambda)$ of $\mathrm{PbI_2}$ films, in addition to optimal values of their average thickness $\bar{d}$ and thickness non-uniformity Δd. The obtained optical constants as a function of wavelength λ in the interference-fringe maxima and minima region (520-900 nm) and in strong absorption region over the whole spectral range studied are plotted as a function of wavelength λ or of the respective photon energy $E_{\mathrm{ph}} = h\nu = hc/\lambda$ $(= 1240/\lambda(\mathrm{nm})$ eV) of light incident on the film to explicate spectral dispersion and inter-bandgap electronic transitions operative in studied flash-evaporated $\mathrm{PbI_2}$ films, as discussed later.

Implementation of the above-described procedures for analyzing the transmittance spectra of our samples F1 and F2 displayed in Fig. 1 was started by choosing an initial guess value of $\Delta d = 25$ nm in the Mathematica program to solve Eq. (4) and Eq. (5) with $\bar{x} = 0$ to find initial values of $n(\lambda_{\mathrm{tang}})$, which are labelled as $n_2(\lambda_{\mathrm{tang}})$ in Table 1 and the values of $\Delta d(\lambda_{\mathrm{tang}})$ depicted in Fig. 4 which are labelled in Table 1 as $\Delta d_{\mathrm{cal}}(\lambda_{\mathrm{tang}})$. This initial value of Δd did not give viable results of subsequent calculations or simulated transmittance spectra, which was then varied until feasible results were achieved. The optimum values of Δd, found to be 14 nm for sample F1 and 14.5 nm for sample F2, were then used to determine more reasonable values for refractive index $n(\lambda_{\mathrm{tang}})$ and $x(\lambda_{\mathrm{tang}})$ in the weak and medium absorption regions, which are designated as $n_3(\lambda_{\mathrm{tang}})$ and $x_3(\lambda_{\mathrm{tang}})$ in Table 1. The $x_3(\lambda_{\mathrm{tang}})$ values were determined from Eq. (10) using the values of $n_3(\lambda_{\mathrm{tang}})$, $n_s(\lambda_{\mathrm{tang}})$ and $T_\alpha(\lambda_{\mathrm{tang}})$.

However, as discussed above, the last extremes were recalculated to give more viable values for $n(\lambda_{\mathrm{tang}})$ by extrapolating their values in the long-λ region by the use of a 4-constant Cauchy dispersion relation [28-30] and the values of noisy $n_3(\lambda_{\mathrm{tang}})$ data were being replaced with the extrapolated values [42]. In

Table 1, the $n(\lambda_{\text{tang}})$ values found from such extrapolation procedure are denoted by $n_4(\lambda_{\text{tang}})$, which were used to plot $\ell/2$-vs-$n_4(\lambda_{\text{tang}})/\lambda_{\text{tang}}(\text{nm})$ with $\ell = 0, 1, 2, 3, \ldots$, in accordance with Eq. (8), the fit of which for the samples F1 and F2 gave an initial value for m_1 ($\ell = 0$) that was rounded off to integers $m_0 = 7$ and 8 as the first extremes observed in their spectra were maxima. The obtained m_0 was then set constant in Eq. (8) to find improved values for average thickness $\bar{d}$ of their films, which were 1072 nm for sample F1 and 1229 nm for sample F2. These results are shown in Fig. 5, with the values of interference order labelled as m in Table 1. The obtained $\bar{d}$ value and order m were then inserted in Eq. (7) to find a more improved values of $n(\lambda_{\text{tang}})$, labelled as $n_5(\lambda_{\text{tang}})$ in Table 1. The values of $n_5(\lambda_{\text{tang}})$, $n_s(\lambda_{\text{tang}})$ and $T_\alpha(\lambda_{\text{tang}})$ were inserted in Eq. (10) to find $x_5(\lambda_{\text{tang}})$ values, which were then used to evaluate the corresponding values of film absorption coefficient $\alpha(\lambda_{\text{tang}})$ listed in Table 1.

The obtained $n_5(\lambda_{\text{tang}})$-$\lambda_{\text{tang}}$ data was then fitted to a 4-constant Cauchy dispersion relation, the fit formula of which was used to extrapolate the $n(\lambda)$ at shorter wavelengths down to $\lambda = 500$ nm, lying into the strong absorption region and beyond. The final results were then used in Eq. (10) to find the corresponding values of $x(\lambda)$ and hence the matching values of $\alpha(\lambda)$ from the relation $\alpha(\lambda) = -\ln \bar{x}(\lambda)/\bar{d}$, using the above-deduced values of average film thickness $\bar{d}$.

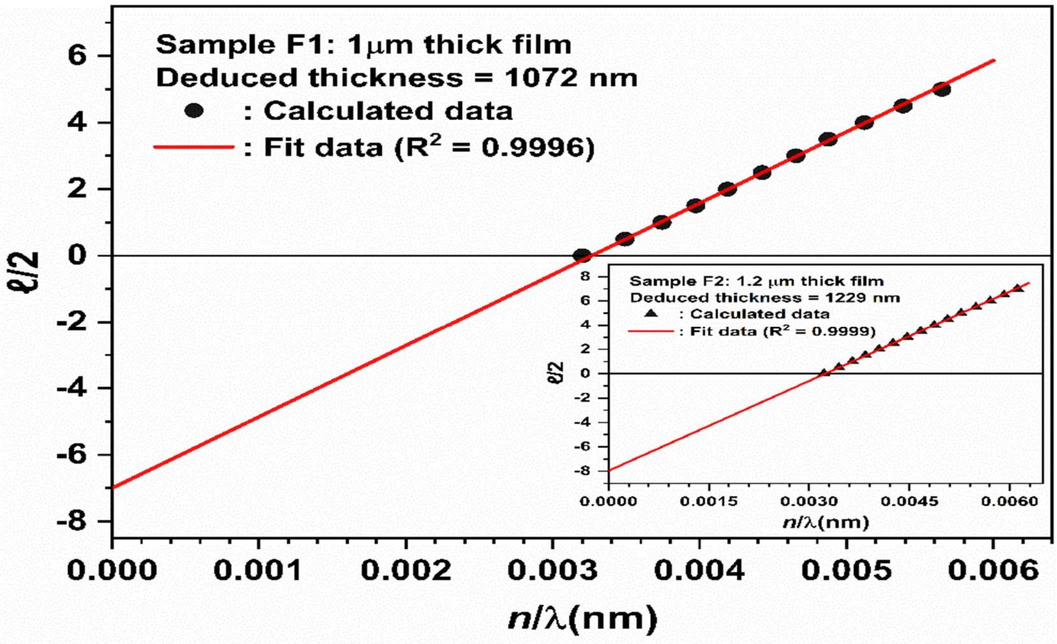

FIG. 5. Plot of $\ell/2$-Vs- n/λ(nm) for samples F1 and F2 of the 1 μm and 1.2 μm thick flash-evaporated PbI_2 films.

TABLE 1. Values of λ, T_M and T_m for the two samples F1 and F2 transmission spectra of Fig. 1; the underlined transmittance values are those calculated by the McClain envelope program. The rest of symbols in the table are explained in the text. The uncertainty in the finally calculated values of the film index of refraction was estimated to be better than 3%, while the uncertainty in the finally calculated average thicknesses of the studied films was around 5%.

Sample	λ (nm)	s	T_M	T_m	n_2	Δd_{cal} (nm)	n_3	x_3	n_4	m	n_5	x_5	α (cm^{-1})
F1 Δd_{opt} = 14 nm $\bar{d}$ = 1072 nm	833	1.585	0.6681	**0.4792**	3.608	40.0	2.666	0.791	2.666	7	2.720	0.791	2184
	776.5	1.588	**0.6512**	0.4647	3.730	36.8	2.711	0.778	2.711	7.5	2.716	0.778	2338
	730.5	1.591	0.6317	**0.4528**	3.857	34.3	2.734	0.762	2.734	8	2.726	0.762	2541
	690.5	1.594	**0.6088**	0.4412	4.004	32.2	2.744	0.740	2.744	8.5	2.737	0.740	2805
	657.5	1.597	0.5870	**0.4296**	4.156	30.4	2.754	0.720	2.754	9	2.760	0.720	3069
	628.5	1.600	**0.5682**	0.4175	4.305	28.5	2.781	0.703	2.781	9.5	2.785	0.703	3284
	604	1.603	0.5499	**0.4053**	4.461	26.9	2.812	0.687	2.812	10	2.817	0.687	3499
	583	1.605	**0.5297**	0.3926	4.640	25.4	2.838	0.669	2.842	10.5	2.855	0.670	3742

Sample	λ (nm)	s	T_M	T_m	n_2	Δd_{cal} (nm)	n_3	x_3	n_4	m	n_5	x_5	α (cm^{-1})
	565	1.608	0.5084	**0.3797**	4.839	24.0	2.860	0.648	2.893	11	2.899	0.653	3983
	549.5	1.610	**0.4857**	0.3651	5.074	22.7	2.890	0.627	2.960	11.5	2.947	0.633	4260
	537	1.613	0.4643	**0.3476**	5.334	21.3	2.965	0.610	3.034	12	3.006	0.613	4559
F2 Δd_{opt} = 14.5 nm $\bar{d}$ = 1229 nm	835.5	1.585	0.6064	**0.4426**	4.004	39.3	2.696	0.731	2.696	8	2.719	0.731	2547
	793	1.587	**0.5998**	0.4346	4.069	36.8	2.736	0.728	2.736	8.5	2.743	0.728	2584
	755	1.589	0.5923	**0.4287**	4.130	34.7	2.759	0.723	2.759	9	2.765	0.723	2642
	722	1.592	**0.5845**	0.4230	4.193	32.9	2.779	0.717	2.779	9.5	2.791	0.717	2706
	693	1.594	0.5761	**0.4160**	4.267	31.2	2.809	0.712	2.808	10	2.820	0.712	2770
	667	1.596	**0.5668**	0.4081	4.352	29.6	2.843	0.705	2.843	10.5	2.850	0.705	2841
	644	1.598	0.5564	**0.3994**	4.449	28.1	2.881	0.698	2.881	11	2.883	0.698	2923
	623.5	1.600	**0.5437**	0.3901	4.565	26.8	2.917	0.689	2.917	11.5	2.918	0.689	3034
	605	1.602	0.5296	**0.3802**	4.697	25.5	2.953	0.677	2.953	12	2.954	0.677	3170
	588.5	1.605	**0.5145**	0.3699	4.844	24.4	2.989	0.665	2.989	12.5	2.994	0.665	3320
	574	1.607	0.5004	**0.3597**	4.993	23.3	3.031	0.655	3.031	13	3.037	0.654	3457
	561.5	1.608	**0.4900**	0.3495	5.121	22.2	3.098	0.650	3.090	13.5	3.085	0.644	3585
	550	1.610	0.4781	**0.3397**	5.264	21.3	3.155	0.642	3.144	14	3.133	0.635	3700
	540	1.612	**0.4617**	0.3280	5.461	20.4	3.212	0.629	3.200	14.5	3.186	0.621	3874
	531.5	1.614	0.4364	**0.3125**	5.776	19.3	3.262	0.605	3.255	15	3.244	0.599	4175

The final values of $\bar{d}$, Δd, $s(\lambda)$, $n(\lambda)$ and $\alpha(\lambda)$ determined from the optical analysis of our non-uniform, absorbing flash-evaporated lead iodide films of samples F1 and F2 on the basis of extended version [42, 43] of Swanepoel EM of non-uniform films were inserted in Eq. (2), which was then evaluated numerically at adopted wavelengths to get their simulated transmission curves. The obtained results yielded good match between their measured transmission spectra and the re-generated (simulated) curves, as illustrated in Fig. 6 for the two samples F1 and F2.

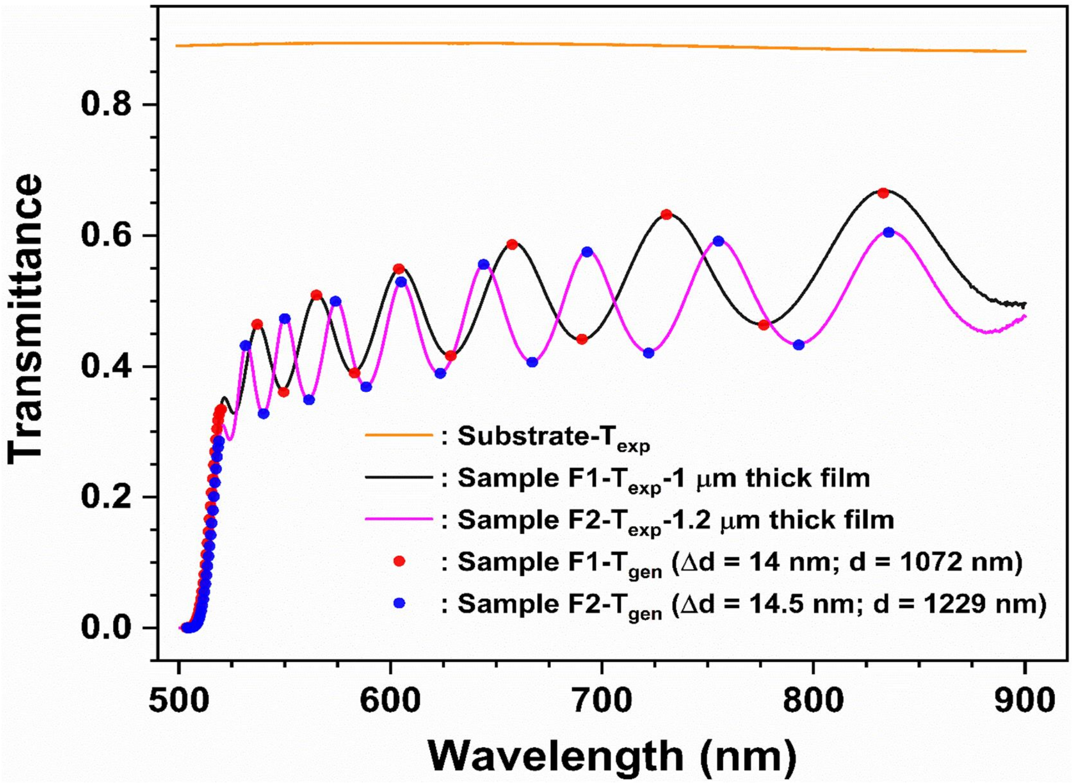

FIG. 6. A plot showing the coincidence of measured transmittance spectra (solid curves) for samples F1 ($\bar{d}$ = 1072 nm) and F2 ($\bar{d}$ = 1229 nm) and their re-generated (simulated) transmission curves and maxima/minima points (solid circles) by integrating numerically Eq. (2) using the attained improved values of their optical constants, their average thicknesses and substrate refractive index n_s over the whole studied wavelength range.

Spectral Dispersion of Refractive Index of Flash-evaporated PbI_2 Films

Fig. 7 illustrates the spectral dispersion of the refractive index $n(\lambda)$ of 1.2 μm thick undoped flash-evaporated PbI_2 film of sample F2 as a function of λ of the light incident on film surface. The plot includes $n(\lambda_{\text{tang}}) - \lambda_{\text{tang}}$ values determined by the extended analytical EM using constructed maxima and minima envelope curves in weak and medium absorption regions and extrapolated $n(\lambda)$ values in the strong absorption region using a fit of a 4-constant Cauchy relation to the finally-improved $n(\lambda_{\text{tang}}) - \lambda_{\text{tang}}$ data. Similar results were found for the 1 μm thick PbI_2 film of sample F1. The inset to Fig. 7 illustrates the validity wavelength range of the Wemple-DiDomenico (WDD) relation that describes the dielectric behavior of a forced-damped single harmonic oscillator [61] above the fundamental absorption edge of the material that is expressed in the following form:

$$[n(\lambda)]^2 = 1 + \frac{E_0 E_d}{E_0^2 - E^2} \tag{11}$$

The oscillator energy E_0 is a measure of the 'average' bandgap energy that is reported to scale with the Tauc bandgap energy E_g^{opt} or the direct bandgap energy E_g of the material as $E_0 = CE_g^{\text{opt}}$, where C is a constant having values in the range 1.5 – 2, depending on the type of material. The oscillator strength E_d is a dispersion energy that is a measure of the average strength of interband optical transition.

Using the obtained fit value of $E_0 = 3.75$ eV, one can obtain $E_g^{\text{opt}} = 2.3$ eV for C = 1.6. The value of E_d determined from the fit of WDD formula to the data chosen in the inset of Fig. 7 was almost near 20.2 eV. These results are in good agreement with the literature findings of other studies on similar flash-evaporated films whose transmission curves were analyzed using rigorous conventional curve-fitting programs [31].

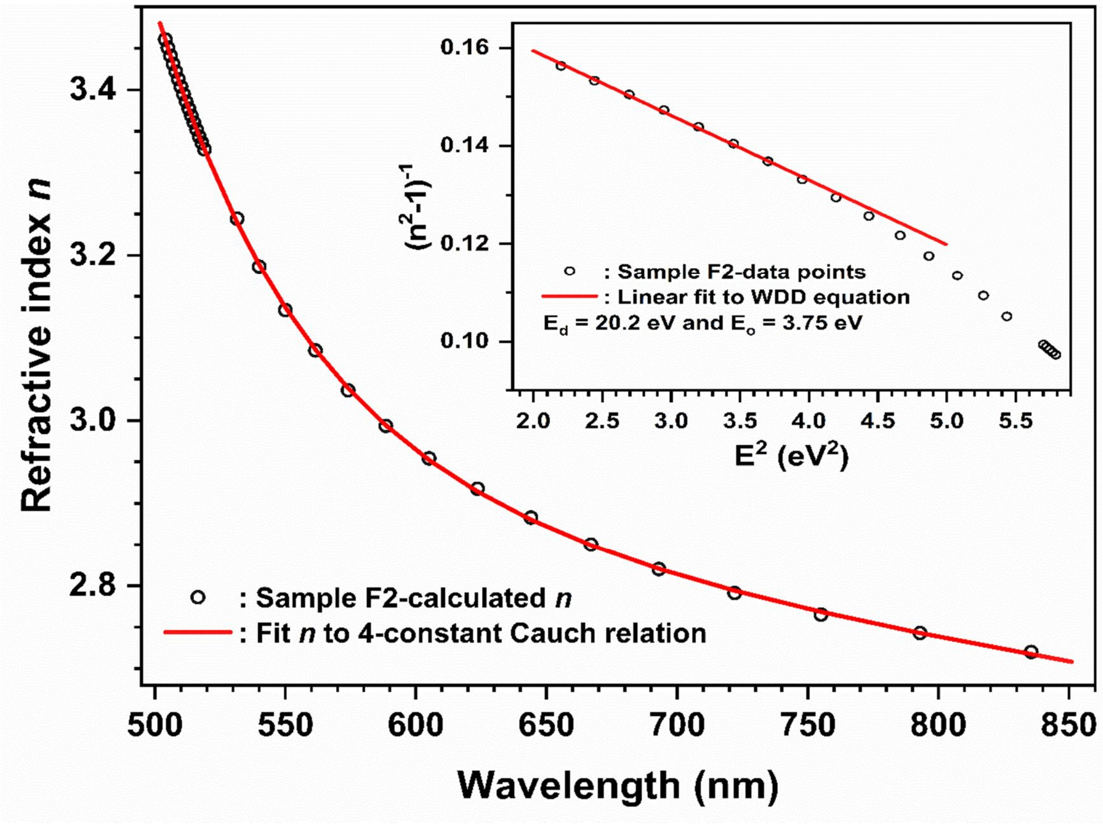

FIG. 7. Spectral dispersion of refractive index $n(\lambda)$ of the 1.2 μm thick flash-evaporated PbI_2 film of sample F2 over the entire weak, medium and strong optical absorption regions. Details of determining $n(\lambda) - \lambda$ data are given in text. Solid curves are curve-fits of $n(\lambda_{\text{tang}}) - \lambda_{\text{tang}}$ data to a 4-constant Cauchy relation. The inset is a fit for the WDD relation.

Determination of Interband Transition Bandgap Energy of Flash-evaporated PbI_2 Films

The variation of absorption coefficient $\alpha(\lambda)$ with photon energy of the light incident on a film specimen below its fundamental absorption edge can be described by simplified expressions that exemplify band-to-band (interband) electronic transitions as given below:

$$\alpha(h\nu) = B\frac{\left(h\nu - E_{\mathrm{g}}\right)^{m}}{h\nu} \quad . \tag{12}$$

The constant B is characteristic of the material, related to the extent of band tailing into the bandgap, E_{g} defines the optical bandgap energy E_{g0} in case of defect-free, perfectly crystalline semiconductors/dielectrics or the Tauc (optical) bandgap energy E_g^{opt} in case of non-crystalline (amorphous) semiconducting materials with disorder that causes broadening of the absorption tail. The numeral exponent m has a variety of values, which depend on the nature of interband optical transition [23, 24, 30, 56-63]. For allowed direct interband transitions, $m = 1/2$, while for Tauc model $m = 2$, which can closely be assigned to allowed indirect phonon-assisted interband transitions.

Fig. 8 illustrates the variation of $\alpha(\lambda)$ of the 1 μm and 1.2 μm thick crystalline, stoichiometric flash-evaporated PbI_2 films of samples F1 and F2 with the photon energy of monochromatic light incident onto them on the basis of interband transition model with $m = 1/2$. The fits are virtuous in the strong absorption region and yield a bandgap energy $E_{\mathrm{g0}} \approx 2.43\,\mathrm{eV}$ (< 3%) for their films, in good agreement with the results of other studies on similar flash-evaporated PbI_2 films [31].

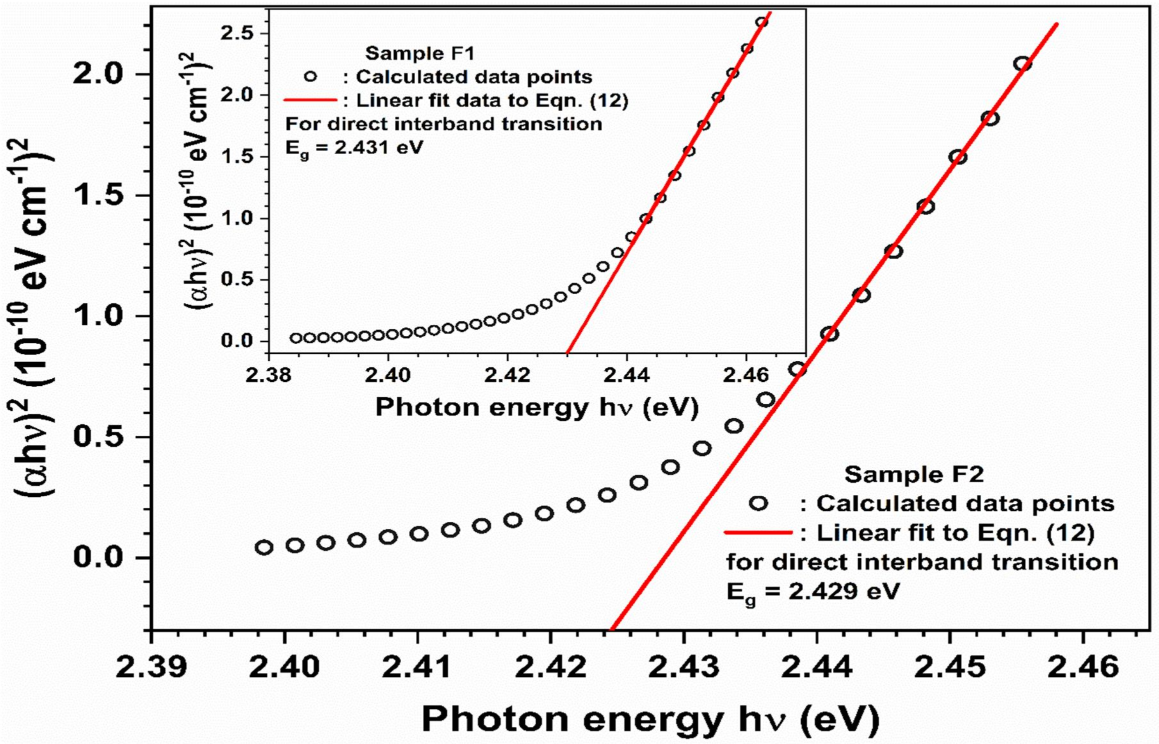

FIG. 8. Variation of absorption coefficient $\alpha(h\nu)$ of the 1 μm and 1.2 μm thick crystalline, stoichiometric flash-evaporated PbI_2 films of samples F1 and F2 with photon energy $(h\nu)$ of light incident onto them in the strong absorption region below the respective fundamental absorption edge. Data is represented by open circles and fits of the linear portions of the $(\alpha h\nu)^2$-Vs- $h\nu$ plots were fitted to Eq. (12) and gave a bandgap energy $E_{\mathrm{g0}} \approx$ 2.43 eV for both films.

Conclusions

Normal-incidence transmission-wavelength $(T_{\exp}(\lambda) - \lambda)$ spectra of 1μm and1.2 μm thick flash-evaporated lead iodide (PbI_2) films deposited on 1.1 mm thick glass slides held at 200 ℃ display well-spaced several interference-fringe maxima and minima in the λ-range 520-900 nm. No transparent region exists at the high λ-side, where the maxima are well below the normal-incidence transmittance T_s of the glass-slides used as substrates for such films. Below 520 nm, the $T_{\exp}(\lambda) - \lambda$ curves decline sharply to zero transmission values (at $\lambda \preccurlyeq 505$ nm) with no significant band-tailing effects, indicating stoichiometric, crystalline-like PbI_2 film absorption. The McClain ENVELOPE algorithm was exploited, with few minor modifications, to construct the maxima $T_M(\lambda_{\max}/\lambda_{\min})$ and minima $T_m(\lambda_{\min}/\lambda_{\max})$ envelope curves from respective $T_{\exp}(\lambda) - \lambda)$ spectra of studied films.

No corrections of the measured (PbI_2 film/substrate} transmittance data for substrate absorption and for spectrometer slit-width effect were made, as they were found to be negligible over the studied λ-range. The observed low transmittance of (PbI_2 film/substrate) system and drastic depression of interference-fringe maxima far below T_s has been related to PbI_2 film thickness non-uniformity (Δd), which causes shrinkage of both maxima and minima, as well as to film optical absorption that reduces both maxima and minima. Thus, application of conventional Swanepoel envelope method (EM) of non-uniform films cannot be used as described by Swanepoel [39], but its extended version suggested by Richards et al. [42, 43] has been adopted.

In the latter optical analysis, values of thickness non-uniformity Δd was varied, in addition to implementing the improvement procedures utilized for determining optical constants of the film under study till a good match between the re-generated (simulated) and measured transmission curves was obtained. Excellent results were achieved from the application of such optical analysis method, which yields plausible values for the average thickness $\bar{d}$ of studied flash-evaporated PbI_2 films, besides their refractive index $n(\lambda)$ and absorption coefficient $\alpha(\lambda)$ in weak, medium and strong absorption regions. The energy-dependence of $\alpha(\lambda)$ is discussed in view of interband electronic transition models and it was found that the direct interband electronic transition model described by Eq. (12) with $m = 1/2$ represents well the variation of $\alpha(h\nu)$ with the photon energy $h\nu$. The value of respective bandgap energy $E_{g0} \approx 2.43$ eV indicates that the produced flash-evaporated PbI_2 films are stoichiometric with 2H-type hexagonal crystallinity, in good agreement with the findings of other studies on similar PbI_2 films the transmission curves of which were analyzed by different means [31].

Acknowledgments

Mousa M. Abdul-Gader Jafar acknowledges The University of Jordan (Amman, Jordan) for offering him the sabbatical leave of absence for the year 2019-2020, during which this manuscript has been completed.

Compliance with ethical standards

Conflict of interest The authors declare that they have no conflict of interest.

References

[1] Moy, J.P., Nucl. Instrum. Meth. A, 442 (2000) 26.

[2] Bennet, P.R., Shah, K.S., Dmitriev, Y., Klugerman, M., Gupta, T., Squillante, M., Street, R., Partian, L., Zantai, G. and Pavlyuchkova, R., Nucl. Instrum. Methods A, 505 (2003) 259.

[3] Zhu, X.H., Wei, Z.R., Jin, Y.R. and Xiang, A.P., Cryst. Res. Tech., 42 (2007) 456.

[4] Green, M.A., Ho-Baillie, A. and Snaith, H.J., Nature Photonics, 8 (2014) 506.

[5] Stranks, S.D. and Snaith, H.J., Nature Nanotechnology, 10 (2015) 391.

[6] Wang, H. and Kim, D.H., Chem. Soc. Rev., 46 (2017) 5204.

[7] Unagami, T., J. Electrochem. Soc., 146 (1999) 3110.

[8] Almalaji, B.R., M.Sc. Thesis, The University of Jordan, (2014), Jordan.

[9] Ghosh, T., Bandyopadhyay, S., Roy, K.K., Kar, S., Lahiri, A.K., Maiti, A.K. and Goswami, K., Cryst. Res. Technol., 43 (2008) 959.

[10] Caldeira Filho, A.M. and Mulato, M., Nucl. Instrum. Meth. A, 636 (2011) 82.

[11] Shkir, M., Abbas, H. and Khan, Z.R., Journal of Physics and Chemistry of Solids, 73 (2012) 1309.

[12] Condeles, J.F. and Mulato, M., J. Mater. Sci., 46 (2011) 1462.

[13] Condeles, J.F. and Mulato, M., J. Phys. Chem. Solids, 89 (2016) 39.

[14] Veissid, N., An, C.Y., Ferreira da Silva, A. and Pinto de Souza, J.I., Mater. Res., 2 (1999) 279.

[15] Ahuja, R., Arwin, H., Ferreira, A., Persson, C., Osorio-Guillen, J.M., Souza de Almeida, J., Moyses Araujo, C., Veje, E., Veissid, N., An, C.Y., Pepe, I. and Johansson, B., Journal of Applied Physics, 92 (2002) 7219.

[16] Matuchova, M., Zdansky, K., Zavadil, J., Tonn, J., Jafar, M.M.A-G., Danilewsky, A.N., Cröll, A. and Maixner, J., Journal of Crystal Growth, 312 (2010) 1233.

[17] Al-Daraghmeh, T.M., Saleh, M.H., Ahmad, M.J.A., Bulos, B.N., Shehadeh, K.M. and Jafar, M.M.A-G., Journal of Electronic Materials, 47 (2018) 1806.

[18] Saleh, M.H., PhD Thesis, The University of Jordan, Amman, (2011), Jordan.

[19] Acuña, D., Krishnan, B., Shaji, S., Sepúlveda, S. and Menchaca, J.L., Bull. Mater. Sci., 39 (2016) 1453.

[20] Kariper, I.A., Opt. Rev., 23 (2016) 401.

[21] AbuEid, M.A., M.Sc. Thesis, The University of Jordan, Amman, (2018) Jordan.

[22] Ward, L., "The optical constants of bulk materials and films", 2nd Ed., (Institute of Physics Publishing, Bristol, UK, 1994).

[23] Born, M. and Wolf, E., "Principles of Optics: Electromagnetic Theory of Propagation, Interference and Diffraction of Light", (Cambridge University Press, Cambridge, 2002).

[24] Dragoman, D. and Dragoman, M., "Optical Characterization of Solids", (Springer-Verlag, Berlin, 2002).

[25] Stenzel, O., "The physics of thin-film optical spectra: An introduction", (Springer, Berlin, 2005).

[26] Chambouleyron, I. and Martínez, J.M., "Optical properties of dielectric and semiconducting thin films; in: Handbook of Thin-film Materials", Ed. Nalwa, H.S., (Academic Press, San Diego, USA, 2001), pp. 593-622.

[27] Jafar, M.M.A-G., European Int. J. Sci. Technol., 2 (2013) 274.

[28] Kasap, S.O., Tan, W.C., Jai Singh, A. and Ray, K., "Fundamental Optical Properties of Materials I; in: Optical Properties of Materials and Their Applications", 2nd Ed., Ed. Jai Singh, (John Wiley & Sons, Ltd., Chichester, West Sussex, 2020), pp. 1-66.

[29] Poelman, D. and Smet, P.F., J. Phys. D: Appl. Phys., 36 (2003) 1850.

[30] Saleh, M.H., Jafar, M.M.A-G., Bulos, B.N. and Al-Daraghmeh, T.M.F., Appl. Phys. Res., 6 (2014) 10.

[31] Jafar, M.M.A-G., Saleh, M.H., Al-Daraghmeh, T.M., Ahmad, M.J.A., AbuEid, M.A., Ershaidat, N.M. and Bulos, B.N., Appl. Phys. A, 125 (2019) 672.

[32] Ventura, S.D., Birgin, E.G., Martínez, J.M. and Chambouleyron, I., J. Appl. Phys., 97 (2005) 043512.

[33] Andrade, R., Birgin, E.G., Chambouleyron, I., Martínez, J.M. and Ventura, S.D., Appl. Optics, 47 (2008) 5208.

[34] Mulato, M., Chambouleyron, I., Birgin, E.G. and Martínez, J.M.., Appl. Phys. Lett., 77 (2000) 2133.

[35] Jafar M.M.A-G., Saleh, M.H., Ahmed, M.J.A., Bulos, B.N. and Al-Daraghmeh, T.M., J. Mater. Sci: Mater. Electron., 27 (2016) 3281.

[36] Swanepoel, R., J. Phys. E: Sci. Instrum., 16 (1983) 1214.

[37] Saleh, M.H., Ershaidat, N.M., Ahmad, M.J.A., Bulos, B.N. and Jafar, M.M.A-G., Opt. Rev., 24 (2017) 260.

[38] González-Leal, J.M., Prieto-Alcon, R., Angel, J-A., Minkov, D.A. and Márquez, E., Appl. Optics, 41 (2002) 7300.

[39] Swanepoel, R., J. Phys. E: Sci. Instrum., 17 (1984) 896.

[40] Ramírez-Malo, J.B., Corrales, R., Márquez, E., Reyes, J. and Fernández-Peña, J.P., Mater. Chem. Phys., 40 (1995) 30.

[41] Nagels, P., Sleeckx, E., Callaerts, R., Márquez, E., González, J.M. and Bernal-Oliva, A.M., Solid State Communications, 102 (1997) 539.

[42] Richards, B.S., MEngSci. Thesis, University of New South Wales, New South Wales, (1998), Australia.

[43] Richards, B.S., Lambertz, A. and Sproul, A.B., Thin Solid Films, 460 (2004) 247.

[44] Márquez, E., Bernal-Oliva, A.M., González-Leal, J.M., Prieto-Alcón, R., Ledesma, A., Jiménez-Garay, R. and Mártil, T., Mater. Chem. Phys., 60 (1999) 231.

[45] Márquez, E., Ramírez-Malo, J.B., Villares, P., Jiménez-Garay, R. and Swanepoel, R., Thin Solid Films, 254 (1995) 83.

[46] Bennouna, A., Laaziz, Y. and Idrissi, M.A., Thin Solid Films, 213 (1992) 55.

[47] Bah, K., Czapla, A. and Pisarkiewicz, T., Thin Solid Films, 232 (1993) 18.

[48] Minkov, D.A., Gavrilov, G.M., Moreno, J.M.D., Vazquez, C.G. and Marquez, E., Meas. Sci. Technol., 28 (2017) 035202.

[49] Minkov, D.A., Gavrilov, G.M., Angelov, G.V., Moreno, J.M.D., Vazquez, C.G., Ruano, S.M.F. and Marquez, E., Thin Solid Films, 645 (2018) 370.

[50] Minkov, D.A., Gavrilov, G.M., Marquez, E., Ruano, S.M.F. and Stoynova, A.V., Optik, 132 (2017) 320.

[51] Ruíz-Pérez, J.J., González-Leal, J.M., Minkov, D.A. and Márquez, E., J. Phys. D: Appl. Phys., 34 (2001) 2489.

[52] Qasem, A., Shaaban, E.R., Hassan, M.Y., Moustafa, M.G. and Hammam, M.A.S., J. Electron. Mater., 49 (2020) 5750.

[53] Shaaban, E.R., Philosophical Magazine, 88 (2008) 781.

[54] Marquez, E., Ramirez-Malo, J.B., Fernandez-Pena, J., Jimenez-Garay, R., Ewen, P.J.S. and Owen, A.E., Opt. Mater., 2 (1993) 143.

[55] McClain, M., Feldman, A., Kahaner, D. and Ying, X., Comput. Phys., 5 (1991) 45.

[56] O'Leary, S.K., Johnson, S.R. and Lim, P.K., J. Appl. Phys., 82 (1997) 3334.

[57] Studenyak, I., Kranjčec, M. and Kurik, M., Inter. J. Optics Appl., 4 (2014) 76.

[58] Jellison, G.E. and Modine, F.A., App. Phys. Lett., 69 (1996) 371.

[59] Forouhi, A.R. and Bloomer, I., Phys. Rev. B, 34 (1986) 7018.

[60] Forouhi, A.R. and Bloomer, I., Phys. Rev. B, 38 (1988) 1865.

[61] Wemple, S.H. and DiDomenico, S., Phys. Rev. B, 3 (1971) 1338.

[62] Tauc, J., “Optical Properties of Amorphous Semiconductors; In: Amorphous and Liquid Semiconductors”, Ed. Tauc, J., (Plenum Press, London, New York, 1974), pp. 159-220.

[63] Zanatta, A.R., Scientific Reports 9 (2019) 11125: 1-12.